Research Article | Vol. 27, No. 12 | 10 Jun 2019 | OPTICS EXPRESS 16791
Optics EXPRESS

Optical direct intensity modulation of a 79GHz resonant tunneling diode-photodetector oscillator

WEIKANG ZHANG,[1,*] SCOTT WATSON,[1] JOSÉ FIGUEIREDO,[2] JUE WANG,[1] HORACIO I. CANTÚ,[3] JOANA TAVARES,[4] LUIS PESSOA,[4] ABDULLAH AL-KHALIDI,[1] HENRIQUE SALGADO,[4] EDWARD WASIGE,[1] AND ANTHONY E. KELLY[1]

[1]*School of Engineering, University of Glasgow, Glasgow G12 8LT, UK*
[2]*Departamento de Física, CENTRA, Faculdade de Ciências da Universidade de Lisboa, Portugal*
[3]*CST-Global Ltd., Hamilton International Tech Park, Hamilton G72 0BN, UK*
[4]*INESC TEC and Faculty of Engineering, University of Porto, Porto, Portugal*
**w.zhang.1@research.gla.ac.uk*

Abstract: We report on the direct intensity modulation characteristics of a high-speed resonant tunneling diode-photodetector (RTD-PD) with an oscillation frequency of 79 GHz. This work demonstrates both electrical and optical modulation and shows that RTD-PD oscillators can be utilized as versatile optoelectronic/radio interfaces. This is the first demonstration of optical modulation of an RF carrier using integrated RTD-PD oscillators at microwave frequencies.

1. Introduction

High-speed optoelectronic radio interfaces are a key technology for high capacity wireless communications. Higher user data rates require a concomitant increase in carrier frequency resulting in systems with tens of Gbps data rates using carrier frequencies of hundreds of gigahertz (GHz) [1–4]. Whilst synthesized multiplier-based systems can be used at high frequencies, the many stages of multiplication result in high power consumption [5] and increased size. An alternative approach is the use of oscillators directly at the carrier frequency, or the use of optical techniques for the generation of the required carrier [6]. We report on an RTD based oscillator which can be data modulated using electrical or optical signals at a carrier frequency of 79 GHz.

RTDs are currently the fastest solid-state electronic device with the highest reported frequency of an RTD oscillator at 1.98 THz [7]. There are several advantages of RTD based technologies, including their simple circuit design and the ability to generate high frequency signals with low energy consumption. The integration of a double barrier quantum well (DBQW) with photodetectors by embedding the DBQW within or adjacent to the light sensitive region gives rise to a new device known as an RTD-PD [8,9]. The RTD-PDs are deemed to be a potential candidate for the low-cost integration of radio and fiber networks.

One of the most important features of an RTD is the N-shaped I-V characteristic due to the resonant tunneling effect, exhibiting a voltage controlled negative differential conductance (NDC) region which provides electrical gain. Thanks to the non-linear electrical and optoelectronic features due to the DBQW structure, the RTD-PD shows an enhancement of photodetection sensitivity, responsivity, detection dynamic range and gain bandwidth-efficiency product values. Optoelectronic applications of resonant tunneling structures for light detection have been proposed in [10,11]. Therefore, it offers the application of simple high frequency electrical oscillators and other optoelectronic devices with new functionalities.

#359354 https://doi.org/10.1364/OE.27.016791
Journal © 2019 Received 6 Feb 2019; revised 10 May 2019; accepted 22 May 2019; published 31 May 2019

Optics EXPRESS

RTD-PDs can operate in two modes: non-oscillating (steady state) or oscillating regimes, depending on the operating point. When biased in the positive differential conductance (PDC) region of the I-V curve, the RTD-PD shows similar functionality to a normal photodetector which can absorb the intensity modulated optical signal and covert it to an electrical signal [12]. When the RTD-PD is biased in the NDC region, it operates in the oscillatory mode which gives rise to an electrical gain and high frequency self-sustained oscillations. Optical modulation characteristics of such an RTD-PD oscillator working in this mode are reported in [13].

In this study, we focus on a specific condition where the RTD-PD is biased at the end of the first PDC region, just before the NDC region, i.e. the interface between the two regions. The input modulated RF signal, injected into the RTD-PD by means of direct electrical or optical intensity modulated subcarrier, shifts the bias operation point from the steady state (PDC region) to the oscillatory state (NDC region) to generate a mm-wave signal that transfers the input data signal onto an RF carrier. An RTD-PD oscillator with a frequency of 79 GHz was characterized with both an electrical and an optical data signal. In principle, this technique can be scaled to higher data rates and higher carrier frequencies and when used with integrated antennae, can result in very low cost, high performance flexible electronic, optical and radio interfaces.

2. Device and experimental set-up

The RTD-PD is a unipolar two-terminal semiconductor device, which corresponds to a vertical stacking of nanometric scale semiconductor epitaxy layers. In this work, the RTD-PD epi-layer was grown on SI-InP, comprising an undoped indium gallium arsenide (InGaAs) layer (5.7 nm) sandwiched between two undoped aluminium arsenide (AlAs) barrier layers (1.7 nm), forming the DBQW structure. The DBQW structure was then surrounded by two 500 nm thick low-doped InGaAlAs spacer layers which act as light absorbing regions. Using low-doped spacer layers here can decrease the device capacitance to improve the frequency response. Furthermore, lowering the doping of collector layers can enhance the electric field which increases the velocity of the photo-generated charge carriers in the collector side, leading to lower transit time and higher photodetection bandwidth. This InP/InGaAlAs system allows the implementation of light detectors that encompass the 1300 nm and 1550 nm optical windows. Then this structure is embedded between two high-doped 300 nm n-type InAlAs layers followed by high-doped InGaAs layers for contact formation. The fabricated size of RTD-PD device is 10 × 10 μm^2, with an optical window of 36 μm^2 to allow direct optical access. A photograph of the device under test is shown in Fig. 1(a). Correspondingly, a schematic circuit structure is represented in Fig. 1(b).

To improve the output power from the oscillator, the proposed RTD-PD oscillator topology utilizes two RTD-PDs connected in parallel. Both RTD-PDs are connected to a shorted 50 Ω coplanar waveguide (CPW) line (L = 130 μm) which provides a resonator inductance required to be resonant with the RTD-PD's self-capacitance for a given oscillation frequency. According to the relationship $f_0 = 1/(2\pi(LC_n)^{1/2})$, where f_0 is the oscillation frequency and C_n is the self-capacitance of RTD, a shorter CPW line is desired to achieve higher oscillation frequencies. Two thin film NiCr stabilizing shunt resistors (R_e = 20 Ω) are used to suppress the low frequency bias oscillation. Two bypassing capacitors (C_e = 50 pF) are used to short-circuit the RF signal to the ground to avoid dissipation of RF power over the stabilizing resistor [14]. There is a block capacitor (C_{block} = 3 pF) on the output side used to prevent any DC leakage flowing into the equipment during the measurement. Comparing to a single-RTD device, ideally this double-RTD oscillator can double the output RF power [15].

Optics EXPRESS

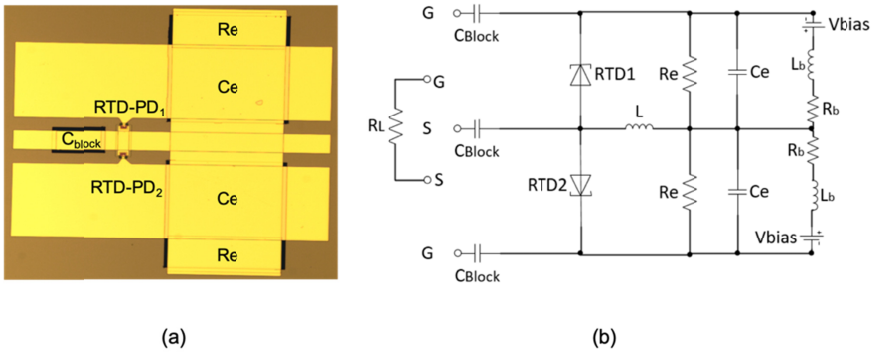

Fig. 1. (a) Photograph of the double RTD-PD oscillator and (b) the schematic circuit structure of the oscillator.

It has been reported that electrical RTD oscillators designed with a slot antenna [16], and oscillation frequencies into the hundreds of GHz, can be employed successfully for THz wireless data transmission by direct modulation at tens of Gbps data rates [3,17]. An electronic based RTD oscillator, with the same circuit design as the one in this work, was also demonstrated for wireless transmission at 300 GHz frequency range with a data rate of up to 7 Gbps [18]. However, an RTD-PD oscillator which can function with both electrical and optical modulated signals for the direct intensity modulation could advance this work further.

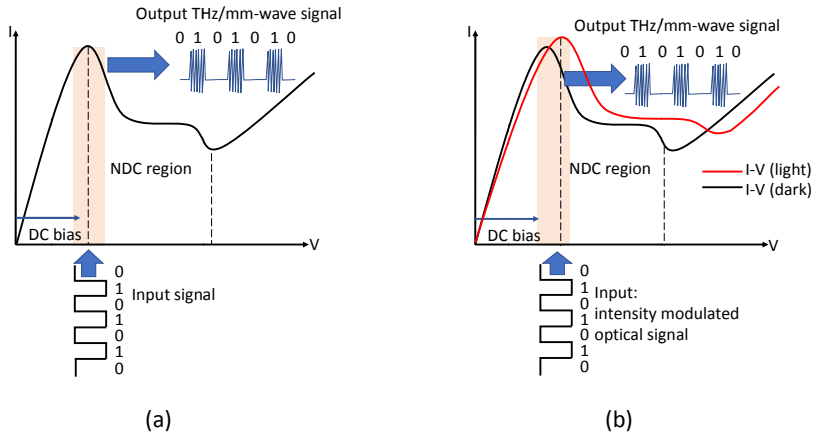

Fig. 2. I-V characteristic of an RTD-PD in the operating condition of (a) electrical modulation and (b) optical modulation.

Firstly, we consider an RTD-PD biased in the first PDC region close to the peak voltage. By superimposing a modulated electrical signal with the DC bias, as schematically shown in Fig. 2(a), the RTD-PD operation point shifts to the NDC region when the DC plus the radiofrequency signal overcomes the peak voltage, making it operate in the oscillatory state. This generates an amplitude modulated THz/mm wave signal whose frequency is determined by the equivalent LC tank of the circuit and the bias voltage.

Due to the RTD-PD photo-detection capabilities, a light signal can also be used to control its operation mode. Injecting an optical signal can shift the RTD-PD global I-V curve to lower or higher voltage, by inducing changes in its effective series resistance which can also lead to an increase in current, and by electron and hole accumulation in the regions contiguous to the DBQW [19]. The direction of the I-V curve shift depends on the location where the photo-charges are generated (in the emitter or collector side of the RTD-PD). The extent of the I-V curve shifting is dominated primarily by the optical power absorbed by the device at a given

Optics EXPRESS

bias voltage, being more pronounced when the device is biased in the first PDC region close to the NDC region. The devices being considered in this work showed a shift to higher voltages, since the injected light is mostly absorbed in the emitter side of the device [13]. When intensity modulated light illuminates the RTD-PD biased in the first PDC region close to the NDC region, its operation point may enter the NDC region because of the light induced I-V curve shift, as schematically represented in Fig. 2(b).

Figure 3 and Fig. 4 illustrate the schematic diagrams of the electrical and optical signal injection experiments respectively. In both cases the RTD-PD oscillator was biased by landing a ground-signal-ground (GSG) probe on the DC port of the oscillator. In the case of the electrical signal injection, the input signal, modulated with a Pseudo Random Binary Sequence (PRBS) pattern at data rates controlled by the signal generator, was fed into the DC port through a bias T. Another GSG probe was landed on the output port of the oscillator and the received signal could be observed as eye diagrams on the digital communication analyzer (DCA). The nominal 80 GHz bandwidth of the DCA allows direct observation of the RF carrier at 79 GHz without triggering allowing the envelope to be observed. The experimental arrangement for electrical characterization of the RTD-PD is shown in Fig. 3.

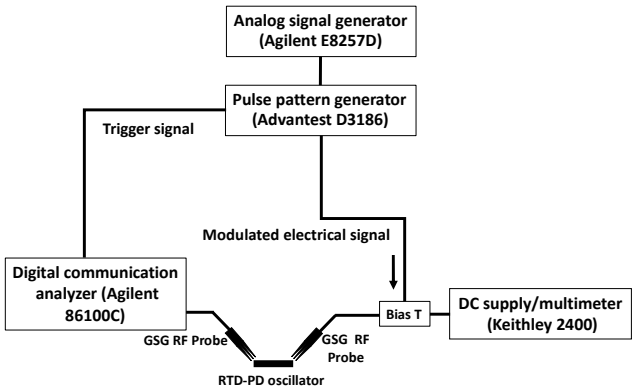

Fig. 3. Experimental set-up for electrical signal modulation.

Figure 4 shows the set-up for the optical signal injection. A laser with a wavelength of 1310 nm was intensity modulated by the PRBS signal generated from the pulse pattern generator. This modulated light wave was amplified by a semiconductor optical amplifier (SOA), and then injected to the RTD-PD via a single mode lensed fiber which was aligned to the top optical window of the RTD-PD. The DC bias voltage and the intensity of the input optical signal were significant to control the absorbed optical power and thus optimize the quality of the eye diagrams.

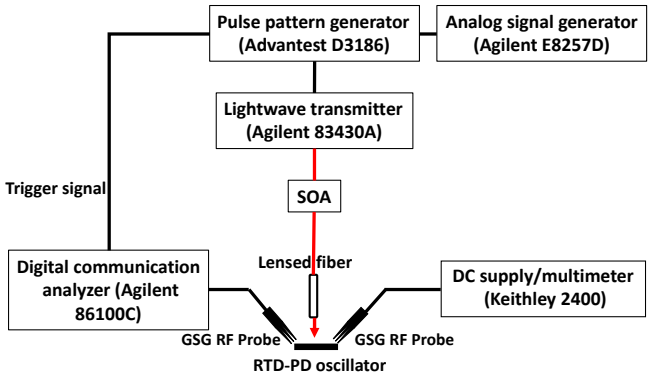

Fig. 4. Experimental set-up for optical signal modulation.

Optics EXPRESS

3. Experimental results

Firstly, electrical signal injection was carried out based on the set-up shown in Fig. 3. The electrical output signal shown in Fig. 5 was obtained from the RF output port of the oscillator when biasing the device in the first PDC region, which is far from the peak voltage, at around 0.7 V. It was observed the PRBS electrical signal injected through the DC port could pass through the oscillator directly. Figures 5(a) and 5(b) represent the output signal for data rates of 400 Mbps and 3 Gbps respectively. The lower frequency patterns are subject to limitations from a high pass capacitor in the circuitry.

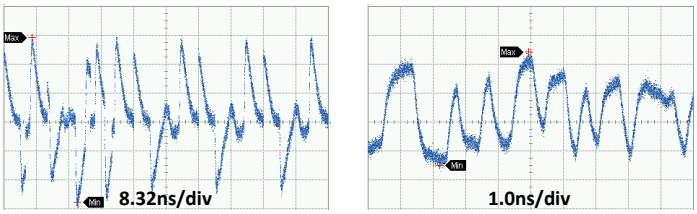

Fig. 5. Output signal from the oscillator at the data rates of (a) 400 Mbps and (b) 3 Gbps when the RTD-PDs were biased in the first PDC region.

Once biasing the RTD-PD close enough to the NDC region, high voltage level signals, i.e. patterns of '1', would drive the RTD into the NDC region resulting in oscillations, whereas a '0' would keep the RTD out with the NDC region and hence, no oscillations. The data rate of the electrical input signal was 100 Mbps. Figure 6(a) shows the output signal whilst biased outside the NDC region at 0.67 V, resulting in no oscillations. The output signals shown in Figs. 6(b) and 6(c) were obtained by biasing at 0.74 V and 0.77 V respectively. It was noticeable that the oscillation overlapped on all the patterns of '1', which conformed to the theoretical expectation in [20]. The performance improves as the DC bias applied approaches the peak of the I-V curve and the device enters into the NDC region.

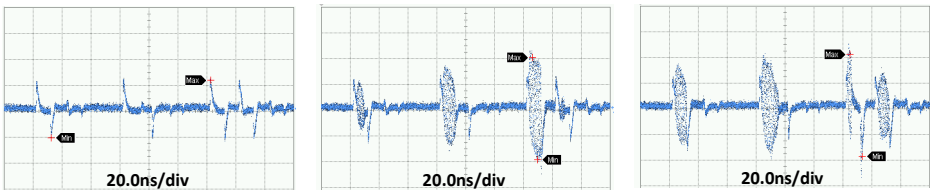

Fig. 6. Output signal from the RTD-PD oscillator when biasing at (a) PDC region (0.67V), (b) NDC region (0.74V) and (c) NDC region (0.77V).

As for the optical modulation experiment, an intensity modulated light-wave illuminated the optical conductive layers via the optical windows. When biasing the RTD in the first PDC region, it worked in the steady-state mode, that is, it behaves like a "normal" (photo-detection without electrical gain) photodetector. Figure 7(a) represents the optical input signal with PRBS waveform at data rate of 50 Mbps used to drive the RTD-PD. The output electrical signal for an RTD-PD biased in the first PDC away from the peak is represented in Fig. 7(b) which has similar features as the results shown in Fig. 6(a). When biasing close enough to the NDC region, high intensity levels in the light-wave signal shifts the RTD-PD operation point into the NDC region. This results in oscillations appearing based on all patterns of '1', as shown in Fig. 7(c).

Optics EXPRESS

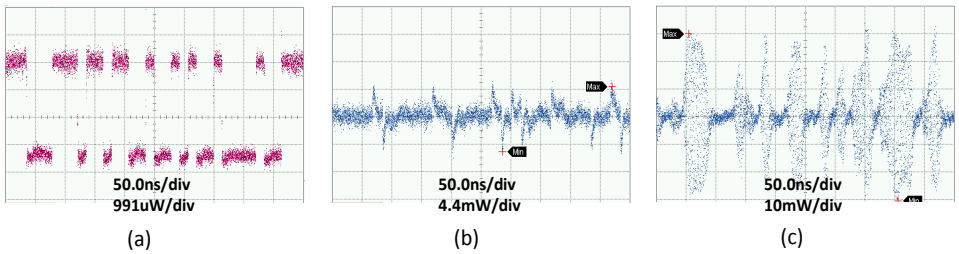

Fig. 7. (a) modulated optical signal injected to the RTD-PD, (b) electrical output signal from the RTD-PD oscillator when biased in the first PDC where is the steady mode, (c) output signal overlapped with oscillation when biasing the RTD-PD from steady state mode into oscillation mode.

4. Discussion

To optimize the quality of the output signal, it is essential to set the bias voltage correctly. This is to ensure all high-voltage level data induces the transition from the first PDC to the NDC making the RTD work in the oscillation mode for each "1" bit. Similarly, it ensures the low voltage level data is still located in the PDC region. It has been observed that not all signals are transmitted equally because of distortion and not all patterns could be presented with oscillation if the bias is inadequate. This phenomenon is noticeable in Figs. 6(b) and 6(c). In Fig. 6(b), it can be seen there is no oscillation on the forth pulse as the bias is 0.74 V, but oscillation appears when bias was increased to 0.77 V shown in Fig. 6(c). We have observed that the RF output power was increased as well due to higher bias. Besides, there are two results if the bias is relatively high, depending on the width of the NDC region. For RTD-PDs with a wide NDC region, biasing beyond the peak voltage may result in the RTD working totally in the oscillation mode; therefore the generated mm-wave is not amplitude modulated by the input signal. The mm-waves generated are frequency modulated ultimately. For RTD-PDs with a relatively narrow NDC region, increasing the bias too much may shift the operation point into the second PDC region, which makes the RTD operate as a photodetector. This is the equivalent of biasing the RTD in the first PDC region, with lower output power due to lower current.

5. Conclusions

Direct optical intensity modulation of a 79 GHz RTD-PD oscillator was demonstrated, and the corresponding electrical modulation was also measured for comparison. Despite the modest data rates for optical modulation of 50 Mbps, this is the first demonstration of optical modulation using an RTD-PD at these frequencies. This preliminary study indicates that these versatile RTD-PD oscillators can potentially be used as an optical transceiver in the interface between optical communication networks and mm-wave/THz terminals. The optimization of the operating conditions is very important to get the best quality output signal. This was achieved by adjusting the bias voltage and controlling the optical power. Higher optical modulation data rates and operation frequencies are expected by optimizing the device design and by improving the experimental set-up in future work.

Funding

European Union's Horizon 2020 iBROW project (645369); European Regional Development Fund (FEDER), Competitiveness and Internationalization Operational Programme (COMPETE 2020) of the Portugal 2020 framework RETIOT project (POCI-01-0145-FEDER-016432).

Optics EXPRESS

References

1. K. Ishigaki, M. Shiraishi, S. Suzuki, M. Asada, N. Nishiyama, and S. Arai, "Direct intensity modulation and wireless data transmission characteristics of terahertz-oscillating resonant tunnelling diodes," Electron. Lett. **48**(10), 582–583 (2012).
2. H.-J. Song and T. Nagatsuma, "Present and Future of Terahertz Communications," IEEE Trans. Terahertz Sci. Technol. **1**(1), 256–263 (2011).
3. N. Oshima, K. Hashimoto, S. Suzuki, and M. Asada, "Wireless data transmission of 34 Gbit/s at a 500-GHz range using resonant-tunnelling-diode terahertz oscillator," Electron. Lett. **52**(22), 1897–1898 (2016).
4. M. Shafi, A. F. Molisch, P. J. Smith, T. Haustein, P. Zhu, P. De Silva, F. Tufvesson, A. Benjebbour, G. Wunder, "5G: A tutorial overview of standards, trials, challenges, deployment, and practice," IEEE J. Sel. Areas Comm. **35**(6), 1201–1221 (2017).
5. I. Kallfass, I. Dan, S. Rey, P. Harati, J. Antes, A. Tessmann, S. Wagner, M. Kuri, R. Weber, H. Massler, A. Leuther, T. Merkle, and T. Kurner, "Towards MMIC-based 300 GHz indoor wireless communication systems," IEICE Trans. Electron. **E98**, 1081–1090 (2015).
6. M. J. Fice, E. Rouvalis, F. van Dijk, A. Accard, F. Lelarge, C. C. Renaud, G. Carpintero, and A. J. Seeds, "146-GHz millimeter-wave radio-over-fiber photonic wireless transmission system," Opt. Express **20**(2), 1769–1774 (2012).
7. R. Izumi, S. Suzuki, and M. Asada, "1.98 THz resonant-tunneling-diode oscillator with reduced conduction loss by thick antenna electrode," in *42nd International Conference on Infrared, Millimeter, and Terahertz Waves* (IEEE, 2017).
8. B. Romeira, L. M. Pessoa, H. M. Salgado, C. N. Ironside, and J. M. Figueiredo, "Photo-detectors integrated with resonant tunneling diodes," Sensors (Basel) **13**(7), 9464–9482 (2013).
9. A. Pfenning, F. Hartmann, F. Langer, M. Kamp, S. Höfling, and L. Worschech, "Sensitivity of resonant tunneling diode photodetectors," Nanotechnology **27**(35), 355202 (2016).
10. J. Figueiredo, B. Romeira, T. Slight, and C. Ironside, "Resonant tunnelling optoelectronic circuits," *Advances in Optical and Photonic Devices* (IntechOpen, 2010).
11. B. Romeira, "Dynamics of resonant tunneling diode optoelectronic oscillators," Thesis, Universidade do Algarve, 2012.
12. W. Zhang, S. Watson, J. Wang, J. Figueiredo, E. Wasige, and A. E. Kelly, "Optical Characteristics Analysis of Resonant Tunneling Diode Photodiode Based Oscillators," in *2018 IEEE 87th Vehicular Technology Conference (VTC Spring)* (IEEE, 2018), pp. 1–6.
13. J. Tavares, L. Pessoa, J. Figueiredo, and H. Salgado, "Analysis of resonant tunnelling diode oscillators under optical modulation," in *2017 19th International Conference on Transparent Optical Networks (ICTON)* (IEEE, 2017), pp. 1–4.
14. J. Wang, L. Wang, C. Li, B. Romeira, and E. Wasige, "28 GHz MMIC resonant tunnelling diode oscillator of around 1mW output power," Electron. Lett. **49**(13), 816–818 (2013).
15. J. Wang, "Monolithic microwave/millimetrewave integrated circuit resonant tunnelling diode sources with around a milliwatt output power," PhD thesis, University of Glasgow, 2014.
16. S. Suzuki, M. Shiraishi, H. Shibayama, and M. Asada, "High-power operation of terahertz oscillators with resonant tunneling diodes using impedance-matched antennas and array configuration," IEEE J. Sel. Top. Quantum Electron. **19**(1), 8500108 (2013).
17. N. Oshima, K. Hashimoto, S. Suzuki, and M. Asada, "Terahertz wireless data transmission with frequency and polarization division multiplexing using resonant-tunneling-diode oscillators," IEEE Trans. Terahertz Sci. Technol. **7**(5), 593–598 (2017).
18. J. Wang, A. Al-Khalidi, C. Zhang, A. Ofiare, L. Wang, and E. Wasige, "Resonant tunneling diode as high speed optical/electronic transmitter," in *2017 10th UK-Europe-China Workshop on Millimetre Waves and Terahertz Technologies (UCMMT)*, (IEEE, 2017).
19. I. Coêlho, J. Martins-Filho, J. Figueiredo, and C. Ironside, "Modeling of light-sensitive resonant-tunneling-diode devices," J. Appl. Phys. **95**(12), 8258–8263 (2004).
20. T. Nagatsuma, "Terahertz communications technologies based on photonic and electronic approaches," 18th European Wireless Conference (IEEE, 2012).